



Published as: *Cell*. 2011 February 18; 144(4): 614–624.

The coding of temperature in the *Drosophila* brain

Marco Gallio^{1,2}, Tyler A. Ofstad^{1,2}, Lindsey J. Macpherson^{1,2}, Jing W. Wang¹, and Charles S. Zuker^{1,2}

¹Departments of Neurobiology and Neurosciences, University of California at San Diego, La Jolla, California 92093-0649, USA

²Departments of Biochemistry and Molecular Biophysics and of Neuroscience, Howard Hughes Medical Institute, Columbia College of Physicians and Surgeons, Columbia University, New York, New York 10032, USA

SUMMARY

Thermosensation is an indispensable sensory modality. Here, we study temperature coding in *Drosophila*, and show that temperature is represented by a spatial map of activity in the brain. First, we identify new TRP channels and demonstrate they function in the fly antenna to mediate the detection of cold stimuli. Next, we identify the hot-sensing neurons and show that hot and cold antennal receptors project onto distinct, but adjacent glomeruli in the Proximal-Antennal-Protocerebrum (PAP) forming a thermotopic map in the brain. We use two-photon imaging to reveal the functional segregation of hot and cold responses in the PAP, and show that silencing the hot- or cold-sensing neurons produces animals with distinct and discrete deficits in their behavioral responses to thermal stimuli. Together, these results demonstrate that dedicated populations of cells orchestrate behavioral responses to different temperature stimuli, and reveal a labeled-line logic for the coding of temperature information in the brain.

INTRODUCTION

The role of our senses is to create an internal representation of the physical and chemical features of the external world. Sight, hearing, touch, smell and taste define the basic palette used by scientists, artists, writers and poets to illustrate how we capture the world in our brains (Shakespeare went even further, and in his Sonnet 141 tells us about the struggles between the senses and the heart). Of course, we now recognize several additional sensory systems, most prominently perhaps temperature sensing.

Recent advances in the study of mammalian thermosensation have provided fundamental insight into molecular mechanisms mediating hot and cold temperature detection (Jordt et al., 2003; McKemy, 2007; Patapoutian et al., 2003). The detection of thermal stimuli relies on receptor proteins activated directly by changes in temperature. At present, four mammalian heat-activated (TRPV1-4) and two cold-activated (TRPM8, TRPA1) ion channels, all members of the Transient Receptor Potential (TRP) family, have been shown to function as temperature receptors. Some of these thermosensors operate in the noxious (TRPV1, TRPV2, TRPA1), and some in the innocuous (TRPV3, TRPV4, TRPM8) temperature range (Basbaum et al., 2009; Caterina et al., 2000; Caterina et al., 1999;

© 2011 Elsevier Inc. All rights reserved.

Publisher's Disclaimer: This is a PDF file of an unedited manuscript that has been accepted for publication. As a service to our customers we are providing this early version of the manuscript. The manuscript will undergo copyediting, typesetting, and review of the resulting proof before it is published in its final citable form. Please note that during the production process errors may be discovered which could affect the content, and all legal disclaimers that apply to the journal pertain.

Caterina et al., 1997; Colburn et al., 2007; Dhaka et al., 2007; Guler et al., 2002; Jordt et al., 2003; Lee et al., 2005; McKemy et al., 2002; Moqrich et al., 2005; Peier et al., 2002a; Peier et al., 2002b; Smith et al., 2002; Story et al., 2003; Xu et al., 2002).

Several cell types are likely to function as peripheral temperature sensors in mammals. Most notably, neurons located in the dorsal root ganglion (DRG) project to the skin, where they detect changes in temperature both in the noxious and innocuous range (Basbaum et al., 2009; Jordt et al., 2003; Patapoutian et al., 2003). TRP channel expression defines at least four DRG neuron sub-classes: TRPV1 expressing (hot nociceptors), TRPV1+TRPA1 expressing (putative hot-cold polymodal nociceptors), TRPM8 expressing (cold sensors), and TRPV2 expressing cells (very high threshold hot nociceptors) (Basbaum et al., 2009; Jordt et al., 2003; McKemy, 2007; Patapoutian et al., 2003). Surprisingly, the “warm receptors” TRPV3 and TRPV4 do not appear to be expressed in DRG neurons, but rather in keratinocytes within the skin (TRPV3; (Peier et al., 2002b), or very broadly in both neural and non-neural tissues (TRPV4; (Plant and Strotmann, 2007). The *in vivo* requirement of TRPs as thermosensors was substantiated by the characterization of knock-out mice lacking TRPV1, TRPV3, TRPV4 or TRPM8 (Caterina et al., 2000; Colburn et al., 2007; Dhaka et al., 2007; Lee et al., 2005; McKemy, 2007; Moqrich et al., 2005). Interestingly, while the phenotypes were often partial and compound supporting a model involving multiple (possibly overlapping) receptors (Lumpkin and Caterina, 2007), some cases were very clear suggesting a 1:1 correspondence between receptor expression and behavior. For example, TRPM8 mutant mice are dramatically impaired in their behavioral and physiological responses to cold temperatures (Bautista et al., 2007; Colburn et al., 2007; Dhaka et al., 2007). As TRPM8 is expressed in most, if not all, cold-sensing neurons (Dhaka et al., 2008; Kobayashi et al., 2005; Takashima et al., 2007) but not in hot nociceptors (Kobayashi et al., 2005), these results suggest that the coding of temperature may be orchestrated by the activity of dedicated cell types, each tuned to respond to a defined temperature range (Lumpkin and Caterina, 2007).

How do animals represent and process thermal stimuli? *Drosophila* provides an attractive system to study temperature coding: flies possess sensory systems anatomically and genetically simpler than those of vertebrates, and critically depend on quick, reliable and robust temperature sensing for survival (an important adaptation of poikilothermic organisms). In *Drosophila*, two related TRP channels have been proposed as temperature receptors: *painless* (Sokabe et al., 2008; Tracey et al., 2003) and *dTRPA1* (Hamada et al., 2008; Kwon et al., 2008; Rosenzweig et al., 2005). The *painless* channel is activated by high, 'noxious' heat (>42–45°C; (Sokabe et al., 2008), and is expressed in peripheral multi-dendritic neurons of the larval body wall (Tracey et al., 2003). As *painless* mutants also fail to react to mechanical injury (Tracey et al., 2003), this channel appears to be required for the function of bimodal thermal/mechanical nociceptors. *dTRPA1* was originally described as a candidate hot receptor based on its ability to respond to warm temperatures in heterologous expression systems (Viswanath et al., 2003). Surprisingly, *dTRPA1* doesn't function in the PNS, but rather in a small cluster of neurons within the brain (Hamada et al., 2008). In addition to internal thermosensors, adult flies have been suggested to have temperature receptors located in antennae (Sayeed and Benzer, 1996; Zars, 2001).

To begin studying temperature coding in *Drosophila*, we isolated mutants affecting behavioral responses to temperature. Here, we describe candidate cold temperature receptors in *Drosophila* and identify the peripheral neurons and the thermosensory organs in which they function. We also used live imaging to record the activity of the peripheral hot and cold thermosensors and studied their function and projections to the brain. Our results substantiate a labeled line wiring logic for cold and hot sensors, and illustrate how the

activity of these dedicated cells may be used to orchestrate an animal's temperature preference.

RESULTS

brivido genes are necessary for behavioral responses to cold temperatures in *Drosophila*

In order to identify potential cold receptors in *Drosophila*, we screened a collection of candidate P-element insertions for altered temperature preference in a simple two-choice assay. Fifteen flies from each P-element line were allowed to distribute in a small arena divided into 4 quadrants, two were set to a reference temperature (25°C), and two to a test temperature (ranging from 11 to 39°C). The time spent by the flies in each quadrant (in a 3 min. trial) was then computed to calculate an avoidance index for the test temperature (see Methods for details). Wild type flies display a clear preference for temperatures in the range of 24–27°C (Sayeed and Benzer, 1996), with robust avoidance to colder and warmer temperatures (Figure 1). One of the candidate lines, however, exhibited a markedly altered behavior, with a clear deficit in their aversion to cold temperatures (NP4486; Figure S1). Interestingly, this line carries a P-element insertion approximately 2 Kb downstream of a predicted Transient Receptor Potential (TRP) ion channel (CG9472; Figure 1). To determine whether this ion channel is in fact involved in thermosensation, we screened for classical loss-of-function mutations within the CG9472 coding region by Tilling (McCallum et al., 2000), and recovered a non-sense mutation (*brv1^{L563>STOP}*) that truncates the protein within the highly conserved ion transporter domain (Figure 1; (Bateman et al., 2000). *brv1^{L563>STOP}* homozygous mutants are viable and display no obvious morphological defects. However, these mutant flies, much like the original NP4486 P-element insertion line, exhibit a selective deficit in their avoidance to cold temperatures (Figure 1). Because of this potential cold temperature sensing deficit, we named CG9472 *brivido-1* (*brv1*, Italian for shiver).

Brv1 is a member of the TRPP (polycystin) subfamily of TRP ion channels (Montell et al., 2002). The *Drosophila* genome encodes two additional uncharacterized TRPPs, CG16793 and CG13762 (here named *brivido-2* and *-3*; Figure 1). Thus, we set out to test if one or both of these TRP genes might be important for thermosensation. Using Tilling, we screened for potential loss of function mutations in *brv2*, and recovered several mutants, including one that carries a non-sense mutation that truncates the protein before the ion transporter domain (*brv2^{W205>STOP}*). Figure 1 shows that *brv2* mutants display dramatic deficits in their avoidance to cold temperatures, even as low as 11°C. Importantly, this defect is due to the loss of the *brv2* TRP channel, as introduction of a wild type gene completely restores normal temperature preference to the mutant flies (Figure S1). *brv3* maps to the X chromosome, and was therefore not amenable to Tilling using the existing mutant collections (Koundakjian et al., 2004). Hence, we targeted an inducible *brv3* RNAi transgene (Ni et al., 2009) to all neurons (under the control of the *scratch* promoter, strongly expressed in the PNS; (Roark et al., 1995) and monitored the resulting flies for temperature choice defects. As seen for *brv1* and *brv2* mutants, reducing *brv3* transcript levels (Figure 1 and Figure S1, and see below) also impacted the animal's specific aversion to cold temperatures. Together, these results reveal an important role for the Brivido TRP ion channels in cold temperature sensing, and led us to hypothesize that Brv-expressing cells might function as cold thermosensors in *Drosophila*.

brv1 expression define a new population of antennal cold receptors

Little is known about the identity or location of the cells that act as cold temperature receptors in *Drosophila*. Electrophysiological studies in other insects, however, have singled out the antenna as an important substrate for cold detection (Altner and Loftus, 1985). The

original *brv1* P-element insertion line also functions as an enhancer trap (Hayashi et al., 2002), therefore we used these flies to examine potential sites of *brv1* expression in the antenna. NP4486-Gal4 drives UAS-GFP reporter expression in different sets of cells in the antenna: (a) mechanosensory neurons of the 2nd antennal segment (Figure S2), (b) three ciliated neurons at the base of the arista (Figure 2, open arrowheads), and (c) a small number (~15–20) of neurons in the sacculus region of the 3rd antennal segment (Figure 2, arrowhead). The expression in all 3 sites reflects the expression of the native *brv1* gene as all are labeled in in situ hybridization experiments with an antisense *brv1* probe (Figure S2). Could any of these neurons be the elusive antennal cold receptors? To answer this question, we expressed G-CaMP, a genetically-encoded calcium activity indicator (Nakai et al., 2001; Wang et al., 2003), under the control of NP4486-Gal4 and investigated the functional responses of the *brv1*-expressing antennal neurons to temperature stimulation. To ensure the integrity of the tissue during functional imaging, we used a set up that permits monitoring G-CaMP's fluorescence in real time through the cuticle, yet still maintains single-cell resolution (see Methods). Our results (Figure 2 and Figure S2) demonstrate that *brv1*-expressing neurons, both in the arista and in the sacculus (but not in the 2nd antennal segment, data not shown) respond rapidly, robustly, and selectively to cooling stimuli. Remarkably, these cells are activated by temperature drops as small as $\sim 0.5^{\circ}\text{C}$, and their responses reliably mirror the kinetics and amplitude of the stimulating cold pulse (Figure 2). Importantly, these cells are not activated by hot stimuli (see below).

Do Brvs function together in thermosensation? We have attempted to define the cellular sites of expression for each of the 3 *brv* genes, but have been unable to map the sites of expression for *brv2* and *brv3* (data not shown). However, three pieces of evidence strongly argue that *brvs* are co-expressed in cold sensing neurons. First, loss-of-function of any one of the *brv* genes results in strikingly similar defects in the behavioral responses of adult flies to cold stimuli (Figure 1). Second, targeting *brv3* RNAi to *brv1*-expressing neurons (under the control of NP4486-Gal4) results in a cold sensing deficit comparable to ubiquitous *brv3* RNAi expression (Figure S1, panel h). Third, we imaged cold-induced calcium transients in *brv1* and *brv2* mutant animals. Our results (Figure 2) show that the cold-evoked responses of *brv1*-expressing cells are severely affected in either *brv1* or *brv2* mutant backgrounds. These results demonstrate that *brvs* are required in the same neurons, and further substantiate *brv*-expressing cells in the antenna as cold temperature receptors.

A new population of “hot” receptors

In addition to the three *brv1*-expressing cold-sensing cells, the arista also houses three additional neurons, for a total of six in each arista (Foelix et al., 1989). We reasoned that an ideal temperature sensing-organ should house cold- and hot-sensors, and therefore examined whether these three extra neurons may function as hot temperature receptors. To sample the activity of the six neurons in the same preparation, we engineered flies expressing G-CaMP in all aristal neurons under the control of the pan-neural driver *elav-Gal4* (Lin and Goodman, 1994), and monitored their responses to cold- and hot temperature stimuli. All six aristal neurons indeed responded selectively to temperature changes: 3 neurons exhibited calcium increases to warming, but not cooling, and 3 to cooling but not warming stimuli (Figure 3). Much like the *brv*-expressing cold receptor neurons, aristal hot-sensing neurons were activated by temperature increases as small as $\sim 0.5^{\circ}\text{C}$, and their responses closely tracked the temperature stimulus (Figure S3). Interestingly, each population was inhibited by the opposite thermal stimuli, with hot cells displaying a decrease in $[\text{Ca}^{++}]_i$ in response to cold stimuli, while the cold cells exhibit a decrease in $[\text{Ca}^{++}]_i$ in response to hot stimuli (Figure 3). Hence, the antenna contains two distinct sets of thermoreceptors that together operate as opposite cellular sensors: one set of cells that is activated by a rapid rise in

temperature but is inhibited by cold stimuli, and another that is activated by cold temperature but is inhibited by hot stimuli (Figure 3).

Recently, another TRP ion channel, dTRPA1, has been proposed to function as a warmth receptor in a small group of neurons in the *Drosophila* brain (i.e. an internal brain thermosensor; (Hamada et al., 2008). Thus, we examined whether *dTRPA1* plays a role in the responses of the antennal hot sensing cells by recording the thermal-induced activity of these neurons in a *dTRPA1* mutant background. Our results demonstrated no significant differences in hot responses between wild type and mutant animals (Figure S3), thus ruling out a significant role for *dTRPA1* in the detection of hot temperature by the antenna.

Distinct brain targets for hot and cold thermoreceptors

How is the antennal temperature code relayed to the brain? Do hot and cold channels converge onto the same target, or do they project to different brain regions? To address these questions, we tracked the projections of the antennal thermoreceptors to the brain. To follow the projections of the cold receptors, we expressed a membrane targeted GFP (CD8:GFP) under the control of the *brv1* enhancer trap, NP4486-Gal4. Because NP4486 is also expressed in the brain (Figure S2), we relied on an intersectional strategy to restrict expression of NP4486-Gal4 only to antennal neurons (e.g. using *eyeless*-flippase expressed in the antenna but not in the brain, and a *FRT*>Gal80>*FRT* transgene; see Methods for details). Figure 4 shows that projections from *brv1* expressing cold-sensing neurons converged onto a previously uncharacterized region of the fly brain, arborizing into a discrete glomerulus lying at the lateral margin of the Proximal Antennal Protocerebrum (PAP).

What about the hot receptors? In order to track the projections of the “hot” arista neurons, we had to first identify selective drivers for these cells. We screened Gal4 lines for reporter expression in the arista and tested candidate lines on two criteria. On the one hand, positive lines had to drive expression of a GFP reporter in only 3 of the 6 arista cells. On the other hand, these labeled cells should respond to hot but not cold stimuli. Indeed, one line, HC-Gal4, drove CD8:GFP expression in 3 out of the 6 arista thermoreceptors, but not in any other cell in the antenna or CNS. In addition, G-CaMP functional imaging experiments proved that these 3 neurons respond specifically to warming, but not cooling stimuli (Figure S3). Therefore, using HC-Gal4 and CD8:GFP we examined the projections of the hot receptors. Figure 4 demonstrates that hot receptors also target the PAP. Notably, these projections are clearly segregated from those originating in the cold-sensing neurons, converging to a glomerulus that is just adjacent, but not overlapping the one targeted by cold cells (Figure 4). Strikingly, the previously described internal warm receptors (expressing dTRPA1; (Hamada et al., 2008) also send projections to the hot glomerulus (Figure S4). Taken together, these results reveal a thermotopic map of projections in the PAP.

A functional map of temperature representation in the protocerebrum

We reasoned that the topographic map of hot- and cold projections in the PAP would translate into a functional representation of temperature in the brain. Thus, we used two-photon calcium imaging (Denk et al., 1990) to examine activity in the brains of flies expressing G-CaMP under the control of either NP4486-Gal4 or HC-Gal4. Indeed, the PAP glomerulus targeted by the cold neuron projections displayed robust calcium transients in response to cold stimuli, while the PAP glomerulus formed by the projections from the hot neurons was selectively stimulated by hot temperature (Figure 5). Importantly, the activity of cold and hot glomeruli was proportional to the stimulus intensity (Figure 5 and Figure S5) and -as seen in the cell bodies- each glomerulus also responded to the opposite temperature stimuli with a decrease in $[Ca^{++}]_i$. We also expressed G-CaMP pan-neurally (under the

control of *elav-Gal4*) so as to simultaneously image both PAP glomeruli, and examined the responses to hot and cold stimulation. Again, only the two PAP glomeruli responded to thermal stimulation, and displayed a high degree of sensitivity and selectivity: the hot glomerulus was activated exclusively by warming, and the cold one by cooling stimuli (Figure 5). Finally, to validate the antennal thermosensors as the major drivers of PAP activity, we showed that surgical resection of a single antennal nerve dramatically reduced PAP responses on the side of the lesion, while bilateral resection affected responses on both sides of the brain (Figure S5 and data not shown). Together, these results validate a functional temperature map in the brain, and demonstrate that hot and cold stimuli are each represented by a unique spatial pattern of activity in the proximal antennal protocerebrum.

Labeled lines for temperature processing in *Drosophila*

To address how the segregated cold and hot inputs into the PAP might be used to produce temperature choice behavior, we examined the impact of functionally inactivating either the hot- or the cold-sensing neurons by transgenically targeting expression of tetanus toxin light chain to these cells (TeNT is an endopeptidase that removes an essential component of the synaptic machinery, (Sweeney et al., 1995)). We hypothesized that if a comparison of both inputs (responding to hot and cold) is always necessary to determine the fly's preferred temperature, then inactivating either cell type should result in a deficit across temperatures. However, if the hot and cold inputs operate as independent conduits, then altering one input may not affect the animal's behavioral responses to the opposite temperature. To inactivate the cold antennal thermoreceptors, we expressed TeNT under the control of NP4486, again utilizing an *ey-FLP* based intersectional strategy to minimize toxin expression in other brain circuits (see methods for details); to abolish synaptic activity from the hot cells we expressed TeNT under *HC-Gal4*. Our results (Figure 6) demonstrate that silencing either the hot- or the cold-sensing neurons results in a highly selective loss of temperature behavior, with cold-cell inactivation affecting only cold-avoidance, and hot-cell inactivation impacting only behavioral aversion to hot temperatures. Thus, the anatomical separation of hot and cold thermoreceptors at the periphery results in labeled lines for hot and cold which are interpreted largely independently to produce temperature preference behavior.

DISCUSSION

A conserved logic for encoding temperature information at the periphery

The *Drosophila* antenna is a remarkable “hub” for the fly's senses, housing cells specialized in detecting sound, humidity, wind direction, gravity, pheromone and olfactory cues (Ha and Smith, 2009; Kamikouchi et al., 2009; Liu et al., 2007; Sun et al., 2009; Vosshall and Stocker, 2007; Yorozu et al., 2009). Here, we show that the arista and sacculus, two unique structures in the antenna, contain thermoreceptors. The antennal thermosensory cells belong to two functional classes: one is activated by heating (hot receptors) and the other by cooling (cold receptors). Notably, each cell type undergoes not only a rapid, transient increase in calcium responses to the cognate stimulus, but in addition a rapid $[Ca^{++}]_i$ drop to the opposite one (i.e. heat for cold cells and cooling for hot cells). Both classes of neurons respond with high sensitivity to small temperature changes ($<0.5^\circ C$), and their calcium transients scale well with the magnitude of the change, particularly for small stimuli ($\Delta t < 5^\circ C$). Thus, these cells are likely to report most accurately the direction and magnitude of small, sudden changes in temperature. Given that flies are poikilotherms, detecting and reacting to changes in temperature with high sensitivity and speed is vital to the survival of the animal.

Mammalian warm and cold thermoreceptive skin fibers are characterized by robust spontaneous activity (which scale with the absolute temperature over a rather broad range),

and respond with an abrupt increase in firing rate to either a sudden increase (hot receptors) or to a sudden decrease (cold receptors) in temperature. Interestingly, their resting firing rate decreases sharply when challenged by the opposite thermal stimulus (Darian-Smith, 1971; Hensel, 1981). The fly antennal thermosensors appear to have similar properties, with the *caveat* that GCaMP imaging does not allow us to monitor resting firing rates, but rather *changes* in spiking frequency. Thus, we suggest that mammals and flies might use a remarkably similar strategy to encode temperature stimuli at the periphery: the activity of specifically tuned populations of cells signals the direction of the temperature change (hot and cold receptors), and the degree to which they are activated signals the intensity of the change (Lumpkin and Caterina, 2007).

Labeled lines and a map of temperature in the protocerebrum

How is the peripheral temperature 'code' represented in the fly brain? The ability to selectively label defined populations of neurons allowed us to track the projections of the antennal hot and cold receptors directly into the brain, and to image their activity in response to temperature stimuli. Our results showed that the axons of these neurons converge into anatomically and functionally distinct glomeruli in the Proximal Antennal Protocerebrum (PAP). Thus, temperature, like the five classical senses, is represented in a defined brain locus by a spatial map of activity.

Given the segregation of hot and cold signals in the PAP, how do flies choose their preferred temperature to orchestrate behavior? We envision at least two potential scenarios: in one, information from both lines (i.e. hot and cold) is combined somewhere upstream of the PAP to decode temperature signals, generate a temperature reading and trigger the appropriate behavioral responses. Alternatively, the “preferred temperature” might be a default state, in essence a point (or temperature range) defined by the independent activity of two labeled lines each mediating behavioral aversion to temperatures above or below this point (in this case temperatures below 21°C and above 28°C). This push-push mechanism would de-mark the boundaries of the non-aversive (i.e. preferred) temperature range, and thus provide a very robust mechanism for transforming temperature signals into a simple behavioral choice. This model predicts that altering one of the lines should not affect the behavioral response to the other: such manipulation would just re-define the boundaries for the preferred temperature. For example a loss of the cold line would produce flies which are no longer averse to temperature below 21°C, but still retain the 28°C warm limit. Indeed, this is precisely what was observed, suggesting that the preferred temperature may in fact be set by the independent action of each receptor system. Together, these results substantiate a thermotopic map in the fly brain, suggest a “labeled line” organization for temperature sensing, and illustrate how dedicated temperature signals from two independent and opposing sensors (hot and cold receptors) can direct behavior.

EXPERIMENTAL PROCEDURES

Experimental animals and transgenes

The *brv1* NP4486 allele is from the Gal4 enhancer trap database at the DGRC, Kyoto Institute of Technology (Hayashi et al., 2002). It harbors a single, P(GawB) insert 2,249 bp downstream of the CG9472 STOP codon (Hayashi et al., 2002). A single early termination mutation was identified for each *brv1* and *brv2* by Tilling (McCallum et al., 2000): for *brv1* the nucleotide change was T>A at position 1683 from the START codon, resulting in the L563>STOP change in the protein sequence. For *brv2*, we recovered a G>A change at position 754 from the START codon, resulting in the early termination W205>STOP. The temperature preference phenotype of each mutant was also tested in trans to a deletion uncovering the region (Df(3L)Exel9007 for *brv1* and Df(3L)Exel6131 for *brv2*) and was

indistinguishable from that of homozygous mutants (Figure S1 and data not shown): we conclude that these alleles are likely null or strong loss of function mutations. The *brv2* rescue construct was produced by cloning a 4 Kb genomic fragment including the *brv2* coding region into a modified pCasper vector. The hot-cell Gal4 driver line was identified from a collection covering a wide range of candidates with expression in the antennae (Hayashi et al., 2002). To restrict expression of CD8:GFP and TeNT to antennal neurons expressing NP4486, we used the following intersectional strategy: eyFLP is active in the antenna (and in the retina), but not in the brain. *tubP-FRT>Gal80>FRT* drives expression of the Gal4 inhibitor Gal80 ubiquitously, effectively silencing NP4486-Gal4 mediated expression of the transgenes. Only in the antenna, where eyFLP is active, the *FRT>Gal80>FRT* cassette is excised and lost, allowing Gal4-mediated expression. This effectively limits transgene expression to the cells in which both eyFLP and NP4486 are active.

Behavioral assays

All assays were carried out in a room kept at ~24°C, ~40% RH. The temperature gradient arena has been previously described (Sayeed and Benzer, 1996) (Figure S1). For two choice assays (Figure 1 and 6) 15 flies are placed on an arena consisting of four 1" square, individually addressable Peltier tiles (Oven Industries Inc.). In each trial, flies are presented for 3 with a choice between 25°C and a test temperature between 11 and 39°C at 2°C intervals (15 trials total). The position of flies is monitored during each trial to calculate an avoidance index for each test temperature. The avoidance index is defined as $(AI = \#flies\ at\ 25^\circ C - \#flies\ at\ test\ temp) / total\ \#flies$. AI values were compared using t-tests (Figure S1 a,b) or by 2-way ANOVA followed by Bonferroni post-tests when comparing more than 2 groups (F1, Figure S1 and F6). Kolmogorov-Smirnov tests were used to confirm a normally distributed sample. Threshold $p=0.05$. Constant variance of the datasets was also confirmed by computing the Spearman rank correlation between the absolute values of the residuals and the observed value of the dependent variable, by SigmaPlot).

In-situ hybridization and immunohistochemistry

Fluorescent in situ hybridization was carried out as in (Benton et al., 2006) with a *brv1* digoxigenin-labeled RNA probe visualized with sheep anti-digoxigenin (Boehringer), followed by donkey anti-sheep Cy3 (Jackson). We were unable to detect *brv2* or *brv3* expression by ISH. Immunohistochemistry was performed using standard protocols.

Real time PCR

Quantitative PCR was carried out in quintuplicates using Brilliant SYBR Green PCR Master Mix (Stratagene) on a StepOnePlus real-time PCR system (Applied Biosystems) using *brv3* specific primers. Beta-actin served as the endogenous normalization control.

Live imaging and two-photon microscopy

Confocal Images were obtained using a Zeiss LSM510 confocal microscope with an argon-krypton laser. For live imaging through the cuticle, intact heads or whole flies were mounted within a custom-built perfusion chamber covered with a coverslip and imaged through a water-immersion 40X Zeiss objective and a EM-CCD camera (Photonmax, Princeton Instruments). Image series were acquired at 10 frames per second and analyzed using ImageJ and a custom macro written in Igor Pro (Wavemetrics). To image the responses of cold receptor neurons in *brv1* and -2 mutant backgrounds (Figure 2), G-CaMP was expressed in all arista neurons (under *elav-Gal4*) in controls (background-matched) and mutant animals. At the beginning of each experiment, a set of defined hot and cold stimuli ($\Delta t \sim 3^\circ C$) was delivered while imaging on different focal planes to identify the 3 hot and 3

cold cells in each arista (note that the G-CaMP responses of hot cells -including inhibition to cold stimuli- remain normal in *brv1* and *-2* backgrounds). The most optically accessible cold receptor cell in each arista was then imaged responding to various cold stimuli. A maximum of 5 stimuli of different intensities was recorded for each preparation.

For two-photon microscopy, we built a customized system based on a Movable Objective Microscope (MOM) from Sutter (Sutter Inc.) in combination with a ultrafast Ti:Sapphire laser from Coherent (Chameleon). Live imaging experiments were captured at four frames per second with a resolution of 128×128 pixels. Analysis of imaging data and $\Delta F/F$ calculations were performed using Igor Pro and a custom macro as in (Wang et al., 2003). For live imaging of PAP projections, fly heads were immobilized in a custom built perfusion chamber. Sufficient head cuticle and connective tissue was removed to allow optical access to the PAP. Temperature stimulation was achieved by controlling the temperature of the medium, constantly flowing over the preparation at 5ml/min, by a custom-built system of 3 way valves (Lee Instruments, response time 2ms). In all experiments, heating or cooling was at $\sim 1^\circ\text{C}/\text{sec}$. Temperature was recorded using a BAT-12 electronic thermometer equipped with a custom microprobe (time constant .004 seconds, accuracy 0.01°C , Physitemp).

Supplementary Material

Refer to Web version on PubMed Central for supplementary material.

Acknowledgments

We thank Cahir O'Kane for UAS-TeNT flies, Paul Garrity for dTRPA1^{KO} flies, and specially Michael Reiser for invaluable help with designing and implementing the behavioral arenas and assays. We also thank David Julius and Avi Priel for their help and kindness hosting us (MG) in our efforts to express Brv channels in *Xenopus* oocytes. Wilson Kwan, George Gallardo and Lisa Ha provided expert help with fly husbandry. We are grateful to Hojoon Lee, Dimitri Trankner and Robert Barretto for help with experiments and data analysis, and Nick Ryba, Michael Reiser and members of the Zuker lab for critical comments on the manuscript. We also thank Kevin Moses, Gerry Rubin and the Janelia Farm Visitor Program. MG was supported by a Wenner-Grens Stiftelse and a Human Frontiers Science Program long term fellowship. LM is a fellow of the Jane Coffin Childs Foundation. CSZ is an investigator of the Howard Hughes Medical Institute and a Senior Fellow at Janelia Farm Research Campus. Author contributions: MG and CZ conceived all the experiments and wrote the paper. MG performed all the experiments presented in this paper, except the in situ hybridizations (TO). TO also helped with the set up for 2-choice behavioral assays and JW helped design and setup the custom imaging system. LJM, MG and TO carried out extensive efforts to heterologously express Brv channels (not shown).

References

- Altner H, Loftus R. Ultrastructure and Function of Insect Thermo- And Hygroreceptors doi:10.1146/annurev.en.30.010185.001421. Annual Review of Entomology. 1985; 30:273–295.
- Basbaum AI, Bautista DM, Scherrer G, Julius D. Cellular and molecular mechanisms of pain. Cell. 2009; 139:267–284. [PubMed: 19837031]
- Bateman A, Birney E, Durbin R, Eddy SR, Howe KL, Sonnhammer EL. The Pfam protein families database. Nucleic Acids Res. 2000; 28:263–266. [PubMed: 10592242]
- Bautista DM, Siemens J, Glazer JM, Tsuruda PR, Basbaum AI, Stucky CL, Jordt SE, Julius D. The menthol receptor TRPM8 is the principal detector of environmental cold. Nature. 2007; 448:204–208. [PubMed: 17538622]
- Benton R, Sachse S, Michnick SW, Vosshall LB. Atypical membrane topology and heteromeric function of *Drosophila* odorant receptors in vivo. PLoS Biol. 2006; 4:e20. [PubMed: 16402857]
- Buchner E, Bader R, Buchner S, Cox J, Emson PC, Flory E, Heizmann CW, Hemm S, Hofbauer A, Oertel WH. Cell-specific immuno-probes for the brain of normal and mutant *Drosophila melanogaster*. I. Wildtype visual system. Cell Tissue Res. 1988; 253:357–370. [PubMed: 2900684]

- Caterina MJ, Leffler A, Malmberg AB, Martin WJ, Trafton J, Petersen-Zeitz KR, Koltzenburg M, Basbaum AI, Julius D. Impaired nociception and pain sensation in mice lacking the capsaicin receptor. *Science*. 2000; 288:306–313. [PubMed: 10764638]
- Caterina MJ, Rosen TA, Tominaga M, Brake AJ, Julius D. A capsaicin-receptor homologue with a high threshold for noxious heat. *Nature*. 1999; 398:436–441. [PubMed: 10201375]
- Caterina MJ, Schumacher MA, Tominaga M, Rosen TA, Levine JD, Julius D. The capsaicin receptor: a heat-activated ion channel in the pain pathway. *Nature*. 1997; 389:816–824. [PubMed: 9349813]
- Colburn RW, Lubin ML, Stone DJ Jr, Wang Y, Lawrence D, D'Andrea MR, Brandt MR, Liu Y, Flores CM, Qin N. Attenuated Cold Sensitivity in TRPM8 Null Mice. *Neuron*. 2007; 54:379–386. [PubMed: 17481392]
- Darian-Smith, ID.; RW. *Peripheral neural mechanisms of thermal sensation*. New York: Appleton-Century Crofts Meredith Corp; 1971.
- Denk W, Strickler JH, Webb WW. Two-photon laser scanning fluorescence microscopy. *Science*. 1990; 248:73–76. [PubMed: 2321027]
- Dhaka A, Earley TJ, Watson J, Patapoutian A. Visualizing cold spots: TRPM8-expressing sensory neurons and their projections. *J Neurosci*. 2008; 28:566–575. [PubMed: 18199758]
- Dhaka A, Murray AN, Mathur J, Earley TJ, Petrus MJ, Patapoutian A. TRPM8 Is Required for Cold Sensation in Mice. *Neuron*. 2007; 54:371–378. [PubMed: 17481391]
- Foelix RF, Stocker RF, Steinbrecht RA. Fine structure of a sensory organ in the arista of *Drosophila melanogaster* and some other dipterans. *Cell Tissue Res*. 1989; 258:277–287. [PubMed: 2510932]
- Guler AD, Lee H, Iida T, Shimizu I, Tominaga M, Caterina M. Heat-evoked activation of the ion channel, TRPV4. *J Neurosci*. 2002; 22:6408–6414. [PubMed: 12151520]
- Ha TS, Smith DP. Odorant and pheromone receptors in insects. *Front Cell Neurosci*. 2009; 3:10. [PubMed: 19826623]
- Hamada FN, Rosenzweig M, Kang K, Pulver SR, Ghezzi A, Jegla TJ, Garrity PA. An internal thermal sensor controlling temperature preference in *Drosophila*. *Nature*. 2008; 454:217–220. [PubMed: 18548007]
- Hayashi S, Ito K, Sado Y, Taniguchi M, Akimoto A, Takeuchi H, Aigaki T, Matsuzaki F, Nakagoshi H, Tanimura T, et al. GETDB, a database compiling expression patterns and molecular locations of a collection of Gal4 enhancer traps. *Genesis*. 2002; 34:58–61. [PubMed: 12324948]
- Hensel, H. *Thermoreception and Temperature Regulation*. London: Academic Press; 1981.
- Jordt SE, McKemy DD, Julius D. Lessons from peppers and peppermint: the molecular logic of thermosensation. *Curr Opin Neurobiol*. 2003; 13:487–492. [PubMed: 12965298]
- Kamikouchi A, Inagaki HK, Effertz T, Hendrich O, Fiala A, Gopfert MC, Ito K. The neural basis of *Drosophila* gravity-sensing and hearing. *Nature*. 2009; 458:165–171. [PubMed: 19279630]
- Kobayashi K, Fukuoka T, Obata K, Yamanaka H, Dai Y, Tokunaga A, Noguchi K. Distinct expression of TRPM8, TRPA1, and TRPV1 mRNAs in rat primary afferent neurons with delta/c-fibers and colocalization with trk receptors. *J Comp Neurol*. 2005; 493:596–606. [PubMed: 16304633]
- Koundakjian EJ, Cowan DM, Hardy RW, Becker AH. The Zuker collection: a resource for the analysis of autosomal gene function in *Drosophila melanogaster*. *Genetics*. 2004; 167:203–206. [PubMed: 15166147]
- Kwon Y, Shim HS, Wang X, Montell C. Control of thermotactic behavior via coupling of a TRP channel to a phospholipase C signaling cascade. *Nat Neurosci*. 2008; 11:871–873. [PubMed: 18660806]
- Lee H, Iida T, Mizuno A, Suzuki M, Caterina MJ. Altered thermal selection behavior in mice lacking transient receptor potential vanilloid 4. *J Neurosci*. 2005; 25:1304–1310. [PubMed: 15689568]
- Lin DM, Goodman CS. Ectopic and increased expression of Fasciclin II alters motoneuron growth cone guidance. *Neuron*. 1994; 13:507–523. [PubMed: 7917288]
- Liu L, Li Y, Wang R, Yin C, Dong Q, Hing H, Kim C, Welsh MJ. *Drosophila* hygrosensation requires the TRP channels water witch and nanchung. *Nature*. 2007; 450:294–298. [PubMed: 17994098]
- Lumpkin EA, Caterina MJ. Mechanisms of sensory transduction in the skin. *Nature*. 2007; 445:858–865. [PubMed: 17314972]

- McCallum CM, Comai L, Greene EA, Henikoff S. Targeted screening for induced mutations. *Nat Biotechnol.* 2000; 18:455–457. [PubMed: 10748531]
- McKemy, DD. Temperature sensing across species. *Pflugers Arch*; 2007.
- McKemy DD, Neuhauser WM, Julius D. Identification of a cold receptor reveals a general role for TRP channels in thermosensation. *Nature.* 2002; 416:52–58. [PubMed: 11882888]
- Montell C, Birnbaumer L, Flockerzi V, Bindels RJ, Bruford EA, Caterina MJ, Clapham DE, Harteneck C, Heller S, Julius D, et al. A unified nomenclature for the superfamily of TRP cation channels. *Mol Cell.* 2002; 9:229–231. [PubMed: 11864597]
- Moqrich A, Hwang SW, Earley TJ, Petrus MJ, Murray AN, Spencer KS, Andahazy M, Story GM, Patapoutian A. Impaired thermosensation in mice lacking TRPV3, a heat and camphor sensor in the skin. *Science.* 2005; 307:1468–1472. [PubMed: 15746429]
- Nakai J, Ohkura M, Imoto K. A high signal-to-noise Ca(2+) probe composed of a single green fluorescent protein. *Nat Biotechnol.* 2001; 19:137–141. [PubMed: 11175727]
- Ni JQ, Liu LP, Binari R, Hardy R, Shim HS, Cavallaro A, Booker M, Pfeiffer BD, Markstein M, Wang H, et al. A *Drosophila* resource of transgenic RNAi lines for neurogenetics. *Genetics.* 2009; 182:1089–1100. [PubMed: 19487563]
- Patapoutian A, Peier AM, Story GM, Viswanath V. ThermoTRP channels and beyond: mechanisms of temperature sensation. *Nat Rev Neurosci.* 2003; 4:529–539. [PubMed: 12838328]
- Peier AM, Moqrich A, Hergarden AC, Reeve AJ, Andersson DA, Story GM, Earley TJ, Dragoni I, McIntyre P, Bevan S, et al. A TRP channel that senses cold stimuli and menthol. *Cell.* 2002a; 108:705–715. [PubMed: 11893340]
- Peier AM, Reeve AJ, Andersson DA, Moqrich A, Earley TJ, Hergarden AC, Story GM, Colley S, Hogenesch JB, McIntyre P, et al. A heat-sensitive TRP channel expressed in keratinocytes. *Science.* 2002b; 296:2046–2049. [PubMed: 12016205]
- Plant TD, Strotmann R. Trpv4. *Handb Exp Pharmacol.* 2007:189–205. [PubMed: 17217058]
- Roark M, Sturtevant MA, Emery J, Vaessin H, Grell E, Bier E. *scratch*, a pan-neural gene encoding a zinc finger protein related to snail, promotes neuronal development. *Genes Dev.* 1995; 9:2384–2398. [PubMed: 7557390]
- Root CM, Semmelhack JL, Wong AM, Flores J, Wang JW. Propagation of olfactory information in *Drosophila*. *Proc Natl Acad Sci U S A.* 2007; 104:11826–11831. [PubMed: 17596338]
- Rosenzweig M, Brennan KM, Tayler TD, Phelps PO, Patapoutian A, Garrity PA. The *Drosophila* ortholog of vertebrate TRPA1 regulates thermotaxis. *Genes Dev.* 2005; 19:419–424. [PubMed: 15681611]
- Sayeed O, Benzer S. Behavioral genetics of thermosensation and hygrosensation in *Drosophila*. *Proc Natl Acad Sci U S A.* 1996; 93:6079–6084. [PubMed: 8650222]
- Smith GD, Gunthorpe MJ, Kelsell RE, Hayes PD, Reilly P, Facer P, Wright JE, Jerman JC, Walhin JP, Ooi L, et al. TRPV3 is a temperature-sensitive vanilloid receptor-like protein. *Nature.* 2002; 418:186–190. [PubMed: 12077606]
- Sokabe T, Tsujiuchi S, Kadowaki T, Tominaga M. *Drosophila* *painless* is a Ca²⁺-requiring channel activated by noxious heat. *J Neurosci.* 2008; 28:9929–9938. [PubMed: 18829951]
- Story GM, Peier AM, Reeve AJ, Eid SR, Mosbacher J, Hricik TR, Earley TJ, Hergarden AC, Andersson DA, Hwang SW, et al. ANKTM1, a TRP-like channel expressed in nociceptive neurons, is activated by cold temperatures. *Cell.* 2003; 112:819–829. [PubMed: 12654248]
- Sun Y, Liu L, Ben-Shahar Y, Jacobs JS, Eberl DF, Welsh MJ. TRPA channels distinguish gravity sensing from hearing in Johnston's organ. *Proc Natl Acad Sci U S A.* 2009; 106:13606–13611. [PubMed: 19666538]
- Sweeney ST, Brodie K, Keane J, Niemann H, O'Kane CJ. Targeted expression of tetanus toxin light chain in *Drosophila* specifically eliminates synaptic transmission and causes behavioral defects. *Neuron.* 1995; 14:341–351. [PubMed: 7857643]
- Takashima Y, Daniels RL, Knowlton W, Teng J, Liman ER, McKemy DD. Diversity in the neural circuitry of cold sensing revealed by genetic axonal labeling of transient receptor potential melastatin 8 neurons. *J Neurosci.* 2007; 27:14147–14157. [PubMed: 18094254]

- Till BJ, Colbert T, Tompa R, Enns LC, Codomo CA, Johnson JE, Reynolds SH, Henikoff JG, Greene EA, Steine MN, et al. High-throughput TILLING for functional genomics. *Methods Mol Biol.* 2003; 236:205–220. [PubMed: 14501067]
- Tracey WD Jr, Wilson RI, Laurent G, Benzer S. *painless*, a *Drosophila* gene essential for nociception. *Cell.* 2003; 113:261–273. [PubMed: 12705873]
- Viswanath V, Story GM, Peier AM, Petrus MJ, Lee VM, Hwang SW, Patapoutian A, Jegla T. Opposite thermosensor in fruitfly and mouse. *Nature.* 2003; 423:822–823. [PubMed: 12815418]
- Vosshall LB, Stocker RF. Molecular architecture of smell and taste in *Drosophila*. *Annu Rev Neurosci.* 2007; 30:505–533. [PubMed: 17506643]
- Wang JW, Wong AM, Flores J, Vosshall LB, Axel R. Two-photon calcium imaging reveals an odor-evoked map of activity in the fly brain. *Cell.* 2003; 112:271–282. [PubMed: 12553914]
- Xu H, Ramsey IS, Kotecha SA, Moran MM, Chong JA, Lawson D, Ge P, Lilly J, Silos-Santiago I, Xie Y, et al. TRPV3 is a calcium-permeable temperature-sensitive cation channel. *Nature.* 2002; 418:181–186. [PubMed: 12077604]
- Yorozu S, Wong A, Fischer BJ, Dankert H, Kernan MJ, Kamikouchi A, Ito K, Anderson DJ. Distinct sensory representations of wind and near-field sound in the *Drosophila* brain. *Nature.* 2009; 458:201–205. [PubMed: 19279637]
- Zars T. Two thermosensors in *Drosophila* have different behavioral functions. *J Comp Physiol [A].* 2001; 187:235–242.

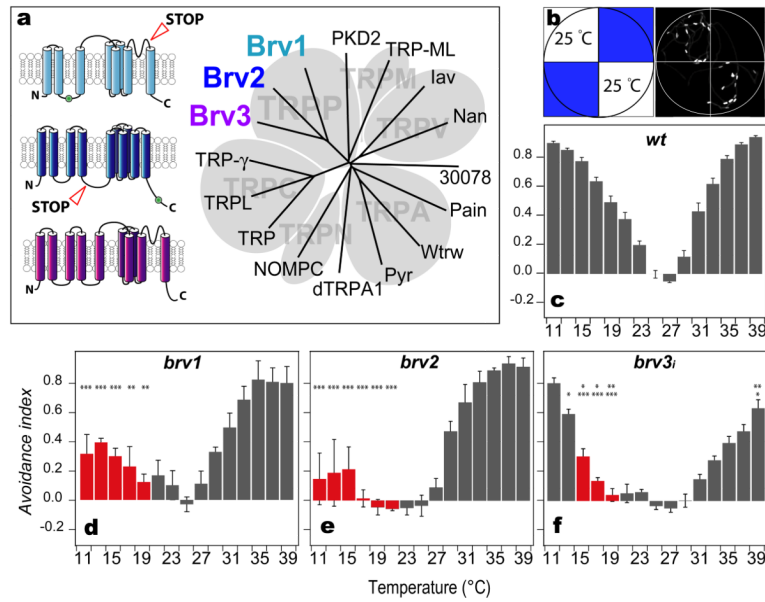


Figure 1. Temperature preference phenotypes of *brivido* mutants

(a) Dendrogram tree of TRP channels in *Drosophila*; *brivido* genes encode 3 members belonging to the TRPP subfamily (Montell et al., 2002). The diagrams to the left illustrate the proposed secondary structure of Brv proteins, and the location of loss-of-function mutations in *brv1* and *brv2* (STOP).

(b,c) Two-choice assay of temperature preference in control flies. (b) Groups of 15 flies are tested in a chamber whose floor is tiled by 4 independently controlled peltier elements. In each trial, a new test temperature (represented in blue) is chosen, and the position of the flies recorded for 180 seconds. Set and reference temperatures are then switched for an additional 3 min trial. (c) Cumulative images of the flies position throughout the trial (illustrated in the right of panel b) are analyzed to compute an avoidance index for each test temperature (grey bars in c, test temperatures varied between 11°C and 39°C, Reference temperature=25°C; n=10, mean±SEM).

(d,e,f) Temperature preference phenotypes of (d) *brv1^{L563>STOP}*, (e) *brv2^{W205>STOP}*, and (f) *scratch-Gal4>brv3(RNAi)* flies (n>5, mean±SEM). Red bars denote AI values significantly different from controls in the cold range (p<0.05). In (f), lower asterisks indicate significant difference from *scratch-Gal4/+* (Figure S1, panel d) and upper asterisks from *+UAS-brv3^{RNAi}* (Figure S1, panel e). In all panels, *** = p<0.001, ** = p<0.01, * = p<0.05, ANOVA. See also Figure S1, panels f-h.

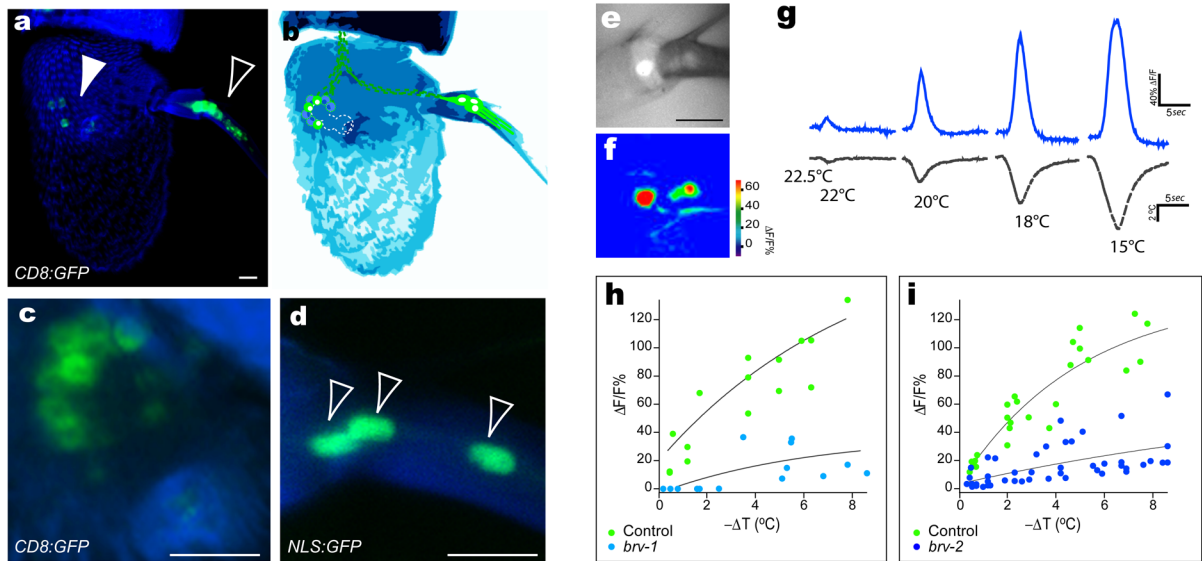


Figure 2. *brv1* and -2 function in cold temperature reception in vivo

(a-d) Cold sensing neurons in the *Drosophila* antenna are revealed by expression of fluorescent reporters under the control of the *brv1* enhancer trap NP4486-Gal4. (a) NP4486-Gal4 drives CD8:GFP expression in neurons located in the sacculus region (arrowhead), and in a small number of neurons at the base of the arista (open arrowhead). (b) *Camera lucida*-style drawing representing the position of the *brv1*-expressing neurons (the sacculus is represented by a dashed line drawing). (c) High-magnification confocal stack showing ~15–20 *brv1*-expressing neurons in the sacculus. (d) An NLS:GFP nuclear localized reporter marks the 3 *brv1*-expressing cells in the arista (open arrowheads).

(e,f) *brv1*-expressing arista neurons respond to cooling stimuli. Shown in (e) is a basal fluorescence image, and (f) the maximal response during a stimulus of $\Delta t \sim 5^\circ\text{C}$ (from 22°C to 17°C), the lookup table represents $\Delta F/F\%$. (g) Temperature responses are reversible and scale with the magnitude of the stimulus (responses of a single cell are shown as blue traces, $\Delta F/F\%$; grey traces denote stimuli in $^\circ\text{C}$; in all panels the scalebar represents $10\ \mu\text{m}$).

(h,i) Loss-of-function mutations in *brivido1* and -2 severely affect the responses of the arista cold-sensing neurons to cooling. Shown are G-CaMP responses from (h) *brv1*^{L563>STOP} (light blue dots, n=5) and (i) *brv2*^{W205>STOP} (dark blue dots, n=10) mutant flies compared to control flies (green dots); G-CaMP was expressed under the pan-neural driver *elav*-Gal4. Each dot represents the response of a single cell to a stimulus; each animal was subjected to a maximum of 5 stimuli of different intensity (see methods, n=5 animals in h and n=10 in i). Note the significant reduction in the responses of mutant animals; we suggest that the small, residual activity seen in each of the mutant lines is likely the result of overlapping function amongst the different *brv* genes (see also Figure S2).

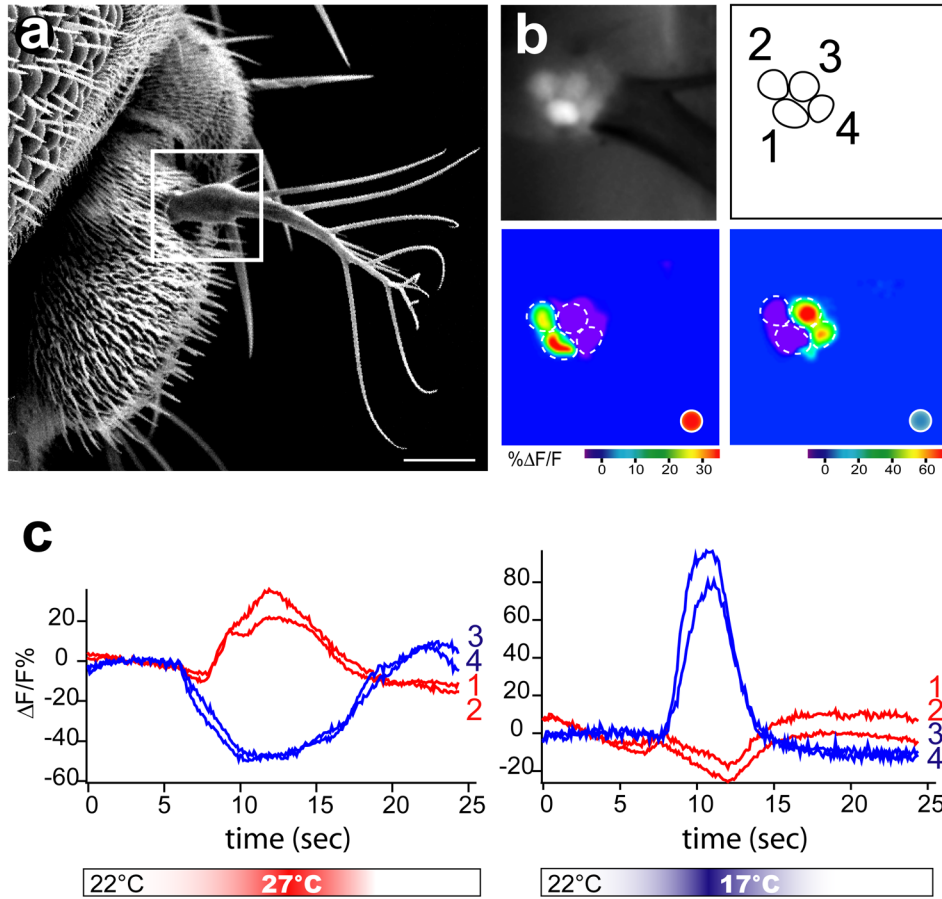


Figure 3. Hot and Cold temperature receptors in the *Drosophila* antenna

(a) Scanning electron micrograph of the *Drosophila* antenna. The arista (white box) houses 6 neurons, 4 of which are visible on the focal plane shown in b. (b) Basal fluorescence and maximal response images of 4 neurons expressing G-CaMP under the control of *elav-Gal4*. Functional imaging reveals that these cells respond to either hot (cells 1 and 2) or cold (cells 3 and 4) thermal stimuli (Stimuli are $\Delta t \sim 5^\circ\text{C}$ from 22°C ; red dot: hot stimulus; blue dot: cold stimulus). (c) Response profile of the two hot- (cells 1 and 2 in panel b) and the two cold-sensing neurons (cells 3 and 4 in panel b) to a stimulus of $\Delta t \sim 5^\circ\text{C}$; red traces denote responses of hot cells, and blue traces depict the cold cells. Note that cold sensing neurons display a drop in intracellular calcium in response to hot stimuli, and the hot-sensing neurons display a decrease in intracellular calcium in response to warming (scalebar represents $20 \mu\text{m}$, see also Figure S3).

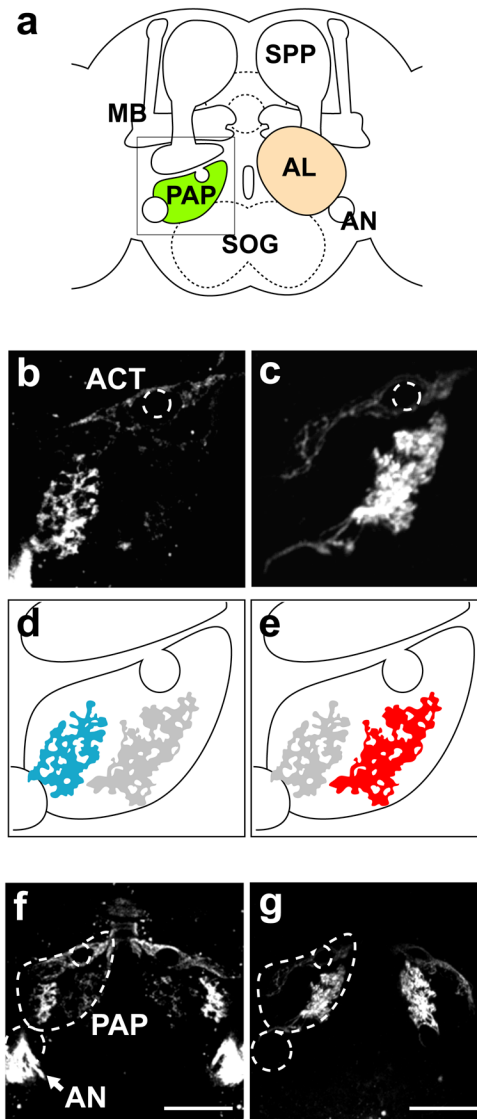


Figure 4. Hot and cold fibers define two distinct glomeruli in the protocerebrum

(a-g) Hot and cold antennal neurons target two distinct, but adjacent glomeruli in the proximal antennal protocerebrum (PAP). (a) Schematic representation of major centers in the fly brain highlighting the position of the PAP (in green). The PAP lies just below the antennal lobe (AL, not shown on the left side of the brain to reveal the PAP); MB, mushroom bodies. SPP: super peduncular protocerebrum. AN: antennal nerve. SOG: sub oesophageal ganglion. (b) PAP projections of antennal cold receptors. NP4486-Gal4 flies carrying *ey-FLP* (active in the antenna) and a *tubulin-FRT>Gal80>FRT* transgene, reveal the projections of cold thermoreceptors to the PAP (see text and methods for details). Cold receptor afferents coalesce into a distinct glomerulus at the lateral margin of the PAP (ACT, antennocerebral tract). (c) Hot receptors (labeled by CD8:GFP driven by HC-Gal4) also target the PAP, forming a similar, but non overlapping glomerulus. (d,e) Schematic illustration of the PAP, with superimposed tracings of the projections shown in panels b and c (blue: cold receptors; red: hot receptors). (f, g) Low magnification confocal stacks showing symmetrical innervation of the PAP. Panel (f) shows a brain from a NP4486-Gal4 fly and panel (g) from a HC-Gal4 animal. The strong labeling seen in the antennal nerve (AN) of

NP4486-Gal4 flies originates in the NP4486-expressing mechanoreceptors of the 2nd antennal segment; these target the Antennal and Mechanosensory Motor Center (AMMC; data not shown; the scalebar represents 50 μ m; see also Figure S4).

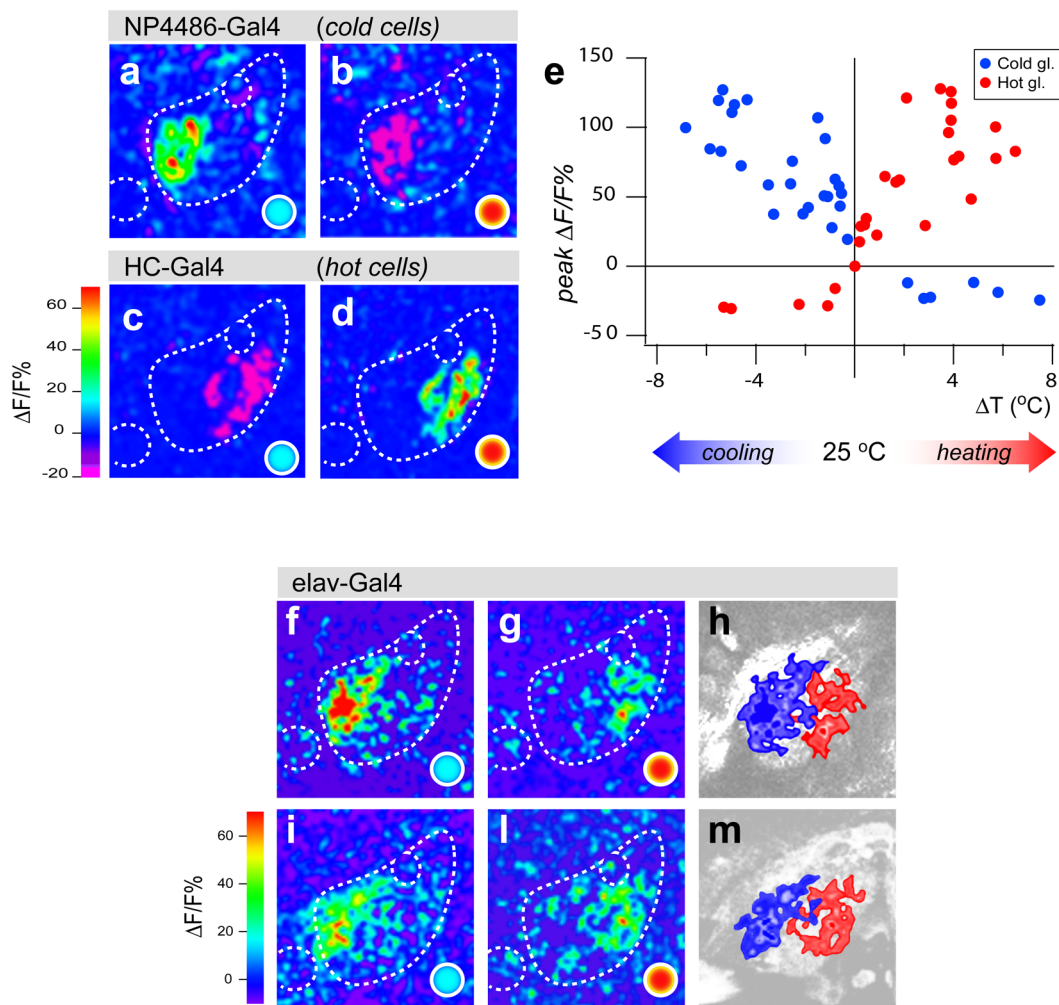


Figure 5. A map of temperature in the PAP

(a) Cold stimulation elicits robust calcium increases in the cold glomerulus, while (b) hot stimulation results in a specific decrease in Ca^{2+} . Conversely, (c) the hot glomerulus is inhibited by cold stimuli, and (d) activated by hot ones; hot and cold stimuli were $\Delta t \sim 5^\circ\text{C}$ from $\sim 25^\circ\text{C}$ (red spot: hot stimulus; blue spot: cold stimulus; G-CaMP was driven under the control of HC-Gal4 or NP4486-Gal4, respectively). (e) Stimulus-response plot representing the responses of hot (red dots) and cold (blue dots) glomeruli. The responses are proportional to the magnitude of the temperature change, with hot glomeruli increasing G-CaMP fluorescence in response to heating stimuli and decreasing it upon cooling. *Vice versa*, cold glomeruli are activated by cooling and appear inhibited by heating stimuli (heating or cooling was from 25°C ; each dot represents the response of a single glomerulus to a stimulus; each animal expressed G-CaMP under the control of HC-Gal4 or NP4486-Gal4, and was subjected to a maximum of 3 stimuli of different intensity, see methods for details, $n=10$).

(f-m) A similar pattern of activity is recorded in the PAP when G-CaMP is expressed throughout the brain using a pan-neuronal driver (elav-Gal4); two independent experiments in two different animals are shown. Note the segregation in the response to cold (f, i) versus hot (g, l) stimuli ($\Delta t \sim 5^\circ\text{C}$ from 25°C). Panels (h, m) are schematic drawings of the superimposed responses in each animal (see also Figure S5).

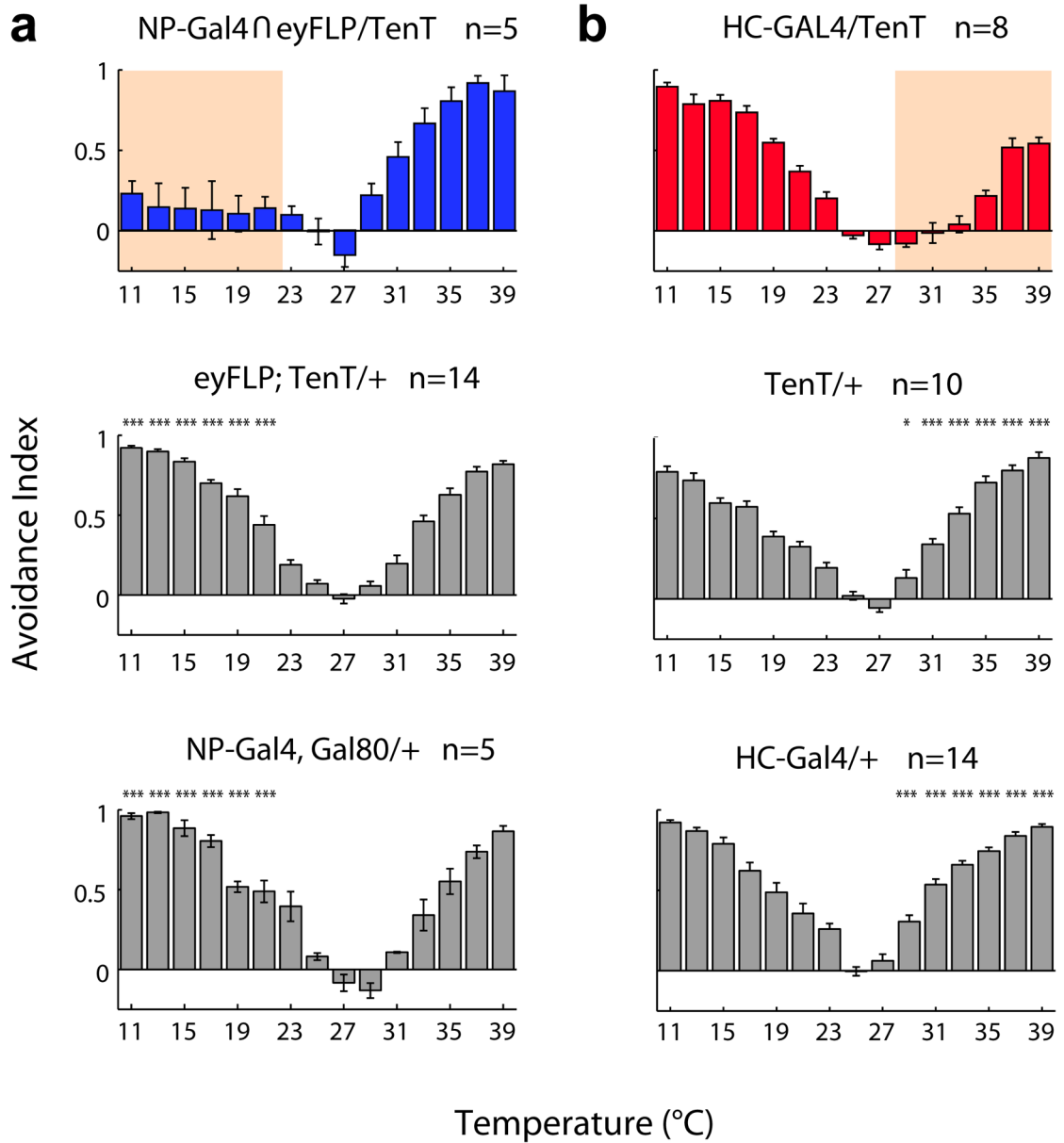


Figure 6. Labeled lines for temperature processing
 (a, b) The behavioral effects of the inactivation of cold and hot thermoreceptors reveal separate channels for the processing of cold and hot temperatures. (a) Expression of tetanus toxin in antennal cold receptors results in significant loss of aversion for temperatures in the 11-23°C range. In contrast, (b) Inactivation of hot receptors results in the reciprocal phenotype, a selective loss of aversion to temperatures above 29°C. Shown below each experimental genotype are the thermal preference records for the parental control lines (gray bars). Pink shading in (a) and (b) highlights AI values significantly different from both appropriate parental strains (n>5, mean±SEM; *** = p<0.001, ** = p<0.01, * = p<0.05, ANOVA, see methods for details).